

Unsupervised Deep Image Hashing through Tag Embeddings

Vijetha Gattupalli
Arizona State University
Tempe, Arizona

vijetha.gattupalli@asu.edu

Baoxin Li
Arizona State University
Tempe, Arizona

baoxin.li@asu.edu

Abstract

Many approaches to semantic image hashing have been formulated as supervised learning problems that utilize images and label information to learn the binary hash codes. However, large-scale labelled image data is expensive to obtain, thus imposing a restriction on the usage of such algorithms. On the other hand, unlabelled image data is abundant due to the existence of many Web image repositories. Such Web images may often come with images tags that contains useful information, although raw tags in general do not readily lead to semantic labels. Motivated by this scenario, we formulate the problem of image hashing as an unsupervised learning problem. We utilize the information contained in the user-generated tags associated with the images to learn the hash codes. More specifically, we extract the word2vec semantic embeddings of the tags and use the information contained in them for constraining the learning. Accordingly, we name our model Unsupervised Deep Hashing using Tag Embeddings (UDHT). UDHT is tested for the task of semantic image retrieval and is compared against several state-of-art unsupervised models. Results show that our approach sets a new state-of-art in the area of unsupervised image hashing.

1. Introduction

Deep learning has instigated note-worthy performance improvement in many supervised computer vision tasks. Image classification [20], object recognition [11] and semantic segmentation [27] are some examples. On similar lines, deep supervised image hashing has also seen significant research in the past few years, recording a remarkable performance improvement as compared to the older non-deep-learning based supervised methods. However, deep unsupervised image hashing has been less attempted and the performance of existing models is still inferior to the non-deep-learning unsupervised methods like ITQ [13].


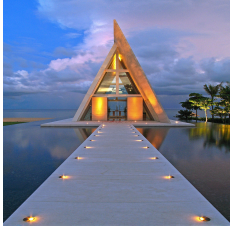

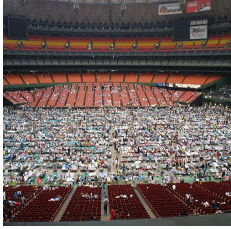

Furthermore, most of the existing unsupervised methods (deep-learning or otherwise) ([13], [30], [34], [9], [25]) fo-

cused on obtaining the hash vectors using the image data only. Much web image data available today have associated textual meta-data (tags). Such tag information is often readily available as opposed to the expensive label information of images. Consequently, *image-tag* pairs are much abundant in quantity as compared to the *image-label* pairs. Owing to these facts, in this paper, we attempt the problem of unsupervised deep hashing by leveraging the tag information associated with the Web images.

The current problem is addressed as unsupervised mainly due to the following reasons. Although image tags may potentially provide semantic information about the image, it is non-trivial to extract explicit label information from raw tags. Table 1 illustrates five randomly picked samples from the NUS-WIDE dataset. It can be noticed that sample1 and sample5 have no tags that are directly associated with the labels "dancing" and "person" respectively. While samples 2 and 3 have some tags that convey label information, they still have their own shortcomings. For example, they are associated with too many uninformative tags, which can be called noise. These uninformative tags may be a consequence of the social-media behaviour of the public like opinion expression, self presentation, attracting attention etc [14]. This results in tags that may be subjective (eg. #thegoldendreams, #handsome, #50faves), purely context oriented (eg. #india, #conradhotel #katrina), photography related (#wideangle) etc. Thus these tags contain information which is not related to the image content, making the process of extracting labels from tags further difficult. There are some prior works [14], [29] that attempted to address the difficulties in extracting information from raw tags.

Further, even if we assume the availability of a model that could explicitly map raw tags to labels, such a model requires the availability of a predefined *label-set* (set of labels used for testing), to learn the mapping from tags to labels. However, such a label-set is in general not explicitly available in a real-world applications like semantic retrieval. Additionally, a real-world problem may involve too huge a number of labels, making it unrealistic to employ super-

Table 1. Table showing the image-tag-label triplets for some random samples from NUS-WIDE dataset. Zoom in to view clearly

	Sample 1	Sample 2	Sample 3	Sample 4	Sample 5
Images					
Tags	#india #cinema #movie #star #still #handsome #bollywood #actor #khan #shahrukh #srk #omshantim	#sunset #bali #reflections #indonesia #mirror #asia #boda #marriage #hochzeit #indonesien #heirat #chappel #conradhotel #50faves #justimagine #weddingchappel #perfectangle #infestyle #megashot #theroadtoheaven #thegoldendreams	#wood #trees #fence #track #derbyshire #farming #wideangle #fields #agriculture #grassland #sigma1020 #autums #marlock #holestone #holestonemoor	#katrina #astrodome #refugees	#shadow #summer #sunny #hat #nycpb #legs #upstate #ps #hires #boating #rowboat #gothamist #strawhat #alita #pawling #saraandthor #littl lakewhaley
Labels	dancing	buildings, clouds, reflection, sky, sunset	grass, sky, tree	none	person

vised algorithms to successfully learn mapping from image space to such huge label set [10]. Thus in a natural setting, it is more meaningful to learn the hash spaces assuming the absence of the label-sets.

Since in this work we focus on learning hash spaces using image-tag pairs only, assuming the unavailability of a pre-defined label set, our approach falls essentially under the category of unsupervised hashing. In testing, we only use the image information as input for retrieval, with the label information being used only for evaluating the retrieval quality.

While our work focuses on using tag information to assist in learning the hash space, our algorithm does not fall under the category of cross-modal hashing (CMH). CMH deals with learning hash spaces that are shared for samples from various modalities. Ideally, a space thus learnt should be able to retrieve samples from one modality by using query samples from a different modality (eg. retrieve images/videos using text queries and vice versa) [32]. Our work only deals with direct image hashing where the query and retrieval samples are images. We only utilize the information from tags to learn better hash spaces for semantic image retrieval. Further, much work in CMH assumes the availability of image-tag-label triplets and use this information to learn the shared hash space. Thus they can be called supervised learning approaches. To the best of our knowledge we haven't found any approach both in the areas of uni-modal image hashing and cross modal hashing, that deal with image-tag pairs in an unsupervised way.

A key component of our method is the utilization of the

word2vec model [28], which is a method for embedding English words onto a vector space such that the cosine similarity between the vectors of the words is in accordance with some semantic similarity of the words themselves. In our task, the image-tags pairs are available from the web-image data-sets, and the tags generally bear some relevance to the semantics of the image (albeit this relevance may be weak, noisy, and incomplete). Hence we employ the *word2vec* representation of the tags in our model, and regularize the learned hash space in such a way that images having similar tag vectors should have similar hash codes.

Using the word vectors of the tags may lead to a better semantic hash space as compared to using the binary tag vectors themselves. This is due to the fact that the word vectors of tags have additional information stored in them that aids the model in learning a more semantically meaningful space. For example, if the training data contains images of cats, dogs, and several other classes, we wish the hash sub-spaces of the cats and the dogs to be close to each other. Then an animal in a test set (for example horse), whose true class is not defined in the training set would be mapped to a hash that falls on the combined sub-space of the cat and the dog. Such arrangement of the sub-spaces although is possible using only the binary tag vectors, the word-vector similarities of the tags when used during the training works as an additional guidance in directing the network towards the desired sub-space. Thus, using the word-vectors of the tags leads to a more semantically meaningful hash space distribution. In the experiments section, we will show the performance difference between using the binary tag vec-

tors and the word vectors of tags to support this rationale.

In summary, this paper attempts the problem of unsupervised image hashing, employing raw image tags through the *word2vec* representation. Our approach demonstrates state-of-art performance on two commonly used datasets MIR-Flickr [17] and NUS-WIDE [5] for the task of semantic image retrieval. In Section 2 we briefly discuss the related work. In Section 3 we introduce our approach. Experiments and results are presented in Section 4. We finally conclude in Section 5.

2. Related Work

Many image hashing algorithms have been proposed under different learning paradigms like supervised hashing, unsupervised hashing, and semi-supervised hashing. Since the main focus of this paper is unsupervised hashing, we only discuss some representative methods in this regard. The foremost image hashing algorithm called the Locality Sensitive Hashing [4] works on the principle of projecting the data on to random hyperplanes and computing each bit based on which half-space the sample falls into. This algorithm is data-independent and therefore the produced hash codes do not capture the structure in the data. Several variants ([6], [22], [3]) have been proposed, all producing hash codes irrespective of the distribution of the data.

Another paradigm of image hashing is the data-dependent hashing methods. Traditionally data-dependent methods have been formulated as independent feature learning and hash coding stages. However, with the advent of deep learning and the huge amount of data available, literature has moved towards learning hash codes as single stage algorithms, which take in image pixels as inputs and directly learn the hash codes. This can also be interpreted as an inbuilt feature learning technique that does not require human intervention. Approaches such as [13], [34], [30] are some representative works of non-deep learning based unsupervised learning. [13] tried to minimize the quantization error between the real-valued uncorrelated feature vector and the binary code by finding a rotation of the zero-centered data. [34] showed the analogy between the problem of finding the optimal hash space distribution and graph partitioning algorithm and attempted the problem using spectral ways. [30] attempted the problem of learning hash spaces in a semi-supervised way by back propagating the classification loss over a limited labeled data-set and an entropy based loss over the entire labelled and unlabelled data-set.

Representative deep-learning-based unsupervised hashing algorithms include [9], [25], [8]. [9] though deep learning based, is not an end-to-end framework that can take in raw images and produce the hashes. They used GIST features as inputs to the neural network and learned the hash codes by minimizing the quantization loss, maximum vari-

ance loss, and the independent bit loss. [25]’s key idea is to produce rotation invariant binary codes and showed that they achieve state-of-art performance on three different tasks namely, image matching, image retrieval and object recognition. [8] learns hash codes as the outputs of the hidden layer of an auto encoder, which they designed to be binary. This makes the learning problem NP-hard and they resort to an alternate optimization scheme to move towards the desired hash space.

Another note-worthy mention in the area of uni-modal image hashing is [1]. They utilized the word embedding of labels as the supervision to learn an image hash space. While this appears similar to our work, they used vector representations of labels, rendering the work to fall under the category of supervised image hashing, whereas our work uses vector representations of raw tags. A common characteristic among most deep learning and non-deep-learning based semantic hashing methods is that they rely only on the information from the images to learn the hash codes, often completely ignoring other associated metadata. Several works in the area of Cross Modal Hashing attempted utilizing tag information along with image data to learn the hash space. However, as mentioned previously, they learn a common hash space for various modalities of input (image and tag in this case), which is different from what we intend to do. Some of the representative works of cross modal hashing include [18], [2], [35]. [18] learns a common hash space for multiple modalities by utilizing deep neural network, thus combining the tasks of feature learning and hash coding into a single framework. [2] intends to align the visual space of images and the semantic space of sentences using language (*word2vec*) and vision (CNN based) models. While this work seems to be similar to the current work, our work attempts to use tag information which is much noisier than the actual English sentences they used in their work. Practically, such clean English sentences are as hard to obtain as the supervised label information. Additionally, both [18] and [2] use the refined label information in their back-propagation, which makes them supervised. [35] learns unified binary codes (in a supervised setting) for various modalities, by formulating a bit by bit optimization scheme to learn the discrete codes directly. An extensive discussion on Cross Modal Hashing and uni-modal hash learning can be found at [32] and [31] respectively.

Taking all the existing work into consideration, we claim that our work stands out from the literature in the notion that the information we use for training (image and tag pairs) are freely available and abundant. Additionally, we propose a way to utilize this information to train a deep learning model, which can later generate hashes for new test images. It should be noted that image-tag pairs are necessary only during the training phase. While testing, the model can generate hash codes using only the image data.

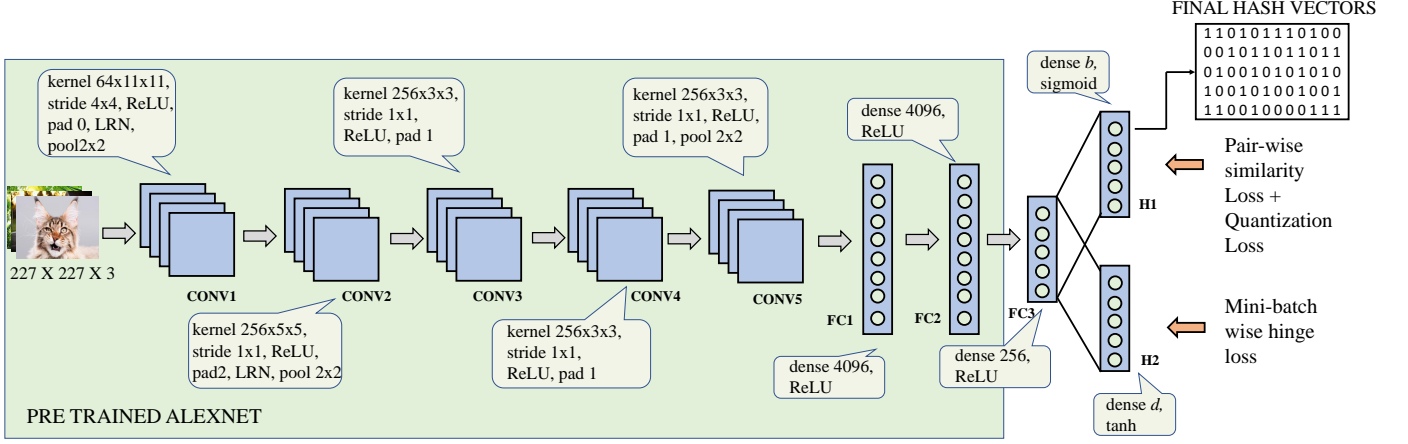


Figure 1. Network Architecture of the proposed model. The outer green box represents the pre-trained AlexNet model; The FC3, H1 and H2 layers are the newly appended layers. The final hash codes are extracted from the H1 layer.

Owing to the above rationale, in the experiments section, we only compare our model to several existing unsupervised image hashing approaches ([13], [34], [30], [30], [19], [15], [37], [26], [8]). All the approaches we consider only take image data as input, while our approach uses both image and tag data to learn the hash space. This is due to the unavailability of any other approach that uses both image and tag information in an unsupervised way. To assist evaluation, we further formulate a baseline and compare our results to this method. The baseline uses both the image and the tag data to learn the hash space. However, it intakes the tag information as binary vectors where as our actual model (UDHT) uses the word embeddings of the tags.

3. Approach

3.1. Problem Formulation

In this work we assume that the data-set has triplets of image-tags-labels $(\mathbf{x}_i, T_i, \mathbf{I}_i)$. Here, \mathbf{x}_i represents the image feature vector for the i^{th} sample, T_i represents the corresponding tags set and \mathbf{I}_i represents its binary label vector. In a generic scenario, each sample is associated with more than one tag and more than one semantic label. Therefore, the tags are represented as a set T_i and the labels are represented as a binary vector \mathbf{I}_i . In the label vector, the value of an element is 1 if the corresponding label is associated with that image and is 0 otherwise. Our task is to find a function $\Psi(\cdot)$ that takes (\mathbf{x}_i, T_i) as inputs and produces a hash vector \mathbf{b}_i as output. The hash space thus learnt should map semantically similar images, defined by the label vectors, to nearby hash codes and dissimilar ones to farther codes. The learning is unsupervised in the sense that it does not assume the availability of the labels. The labels are only employed for evaluating the model in semantic image retrieval.

3.2. Tag Processing

Let τ_i^j represent a tag in the tag set T_i , where j is the index of the tag in the set, i.e., $j \in [1, m]$ where m is the total number of tags associated with the i^{th} sample. We convert each tag τ_i^j into a d -dimensional vector using the *word2vec* language model [28]. Thus for each tag τ_i^j , we obtain a vector representation \mathbf{v}_i^j which is the *word2vec* representation of the tag word τ_i^j . Since each image has multiple tags associated with it, we aggregate all the tag vectors into a single d -dimensional vector for a given image. In this work, we adopted basic functions like *mean* and *idf* (inverse document frequency) to compute the aggregated vector \mathbf{w}_i . In the experiment section, we show that even such basic aggregation techniques lead to significant performance boosts.

The formulae used to compute \mathbf{w}_i are given below.

$$Mean : \mathbf{w}_i = \frac{1}{m} \sum_{j=1}^m \mathbf{v}_i^j \quad \text{and} \quad idf : \mathbf{w}_i = \frac{1}{m} \sum_{j=1}^m \log \frac{N}{n(\tau_i^j)} \mathbf{v}_i^j$$

Here, N represents the total number of tags in the database and $n(\tau_i^j)$ represents the number of images associated with the tag τ_i^j . Additionally, we used only *idf* instead of *tf-idf* (term frequency - inverse document frequency) to weight the vectors as the term frequency term in this scenario will always be 1 (i.e., for any given image each of its tags appears only once in the tag set T_i).

Thus we arrive at the *image - tag vector* $(\mathbf{x}_i, \mathbf{w}_i)$ pairs from the initial *image - tag set* (\mathbf{x}_i, T_i) pairs.

3.3. Designing a Network for Hashing

We use the pre-trained AlexNet model as a key building block for our hashing model. The network takes 227 X 227

X 3 dimensional images as input and passes it through five convolutional layers and two fully connected layers. We call the convolutional layers as CONV_i ($i=1, \dots, 5$), and the fully connected layers as FC1 and FC2. Until the FC2 layer, the architecture is identical to the AlexNet [20] architecture and the weights are initialized to the pre-trained ImageNet [7] weights. The FC2 layer produces a 4096 dimensional vector, which is given as input to another fully connected layer FC3. FC3 outputs 256 dimensional vector which is further fully connected to two layers H1 and H2 in a lateral fashion. The acronyms H1 and H2 represent the *Head1* and *Head2* respectively. The outputs of H1 and H2 are b (number of bits in the hash code) and d (dimensionality of the aggregated tag vector) dimensional vectors, which are then topped by *sigmoid* and *tanh* activations respectively. The entire architecture is shown in Figure 1 where the green box represents the base AlexNet model and the rest represent the proposed layers. The new layers are initialized with *glorot normal* [12] weights.

The model is trained on three loss components back propagating from the two heads H1 and H2 into the network. More specifically, we back propagate pair-wise similarity loss and quantization loss from H1, and mini-batch wise hinge loss from H2. Thus we presume that the loss on H2 (hinge loss) forces the network to form feature spaces (especially at the later layers, H2 and FC3) that are in accordance with the semantic information contained in the aggregated tag vectors, \mathbf{w}_i . On the other hand, the pair-wise loss on H1 aligns the hash space such that semantically similar image pairs are close by and dissimilar pairs are farther. Thus the two main loss components augment each other and guide the network towards learning a semantically meaningful hash space. The third loss component, the quantization loss, forces the output of H1 to be close to 0 or 1.

The pairwise Euclidean loss applied on H1 was first used for hashing in [21] while the quantization loss was first used in [13]. The hinge loss on the head H2 is a ranking loss first used by [10] to learn a semantically meaningful real valued image representation using word embeddings of classification labels. While the hinge loss component does not seem to serve a clear purpose in this network architecture, empirical results show that this component contributes significantly to the performance boost of our model. Also, [10] mentions that using such loss boosts the performance of their model instead of using a $L2$ component. They presume that this could be due to the fact that the problem of forming a semantically meaningful image representation space is a ranking problem in general and therefore such a ranking loss could be more relevant. On similar lines, we can argue that the current problem of learning image hashes is a ranking problem as well, and thus, such a hinge loss component could boost the performance of a retrieval system significantly.

During inference, only H1 is used to extract the features, which are then quantized to obtain the hash code according to the following scheme:

$$\mathbf{b}_i = \frac{1}{2}(\text{sgn}(\mathbf{h}_i^1 - 0.5\mathbf{I}) + 1)$$

Here, \mathbf{h}_i^1 represents the real-valued feature vector obtained at the output of H1, sgn represents a sign function that outputs $1/-1$ based on if the input to the sign function is positive or negative and lastly, \mathbf{I} represents a vector of ones of length b . Thus, we obtain binary codes which have a value of $1/0$ from a raw train/test images.

3.4. Designing the Loss Functions

3.4.1 Pair-wise Similarity Loss

Most state-of-art supervised learning methods assume binary similarity between two images, i.e., two images can be either similar(1) or dissimilar(0) depending on if they share a common label or not. However, in the current unsupervised learning context, we intend to use cosine similarity between the aggregated tag vectors as the ground truth similarity. Since cosine similarity is real-valued and can take values between -1 and 1, we presume the ground truth similarity in our case is not binary valued, i.e., we can deem an image pair to be less similar or more similar, instead of absolutely declaring it to be similar or dissimilar. We only consider this notion of ground truth similarity while training the model and stick with the traditional 0/1 similarity during evaluation. We formulate the pair-wise similarity loss function as follows. For any image pair $(\mathbf{x}_i, \mathbf{x}_j)$, the loss function should push the corresponding hashes closer if the cosine distance between them is smaller and vice-versa. The equation of this loss function is given below,

$$L_1 = \sum_{i=1}^k \sum_{j=1}^k \left[\frac{1}{b} (\mathbf{h}_i^1 - \mathbf{h}_j^1)^T \cdot (\mathbf{h}_i^1 - \mathbf{h}_j^1) - \frac{1}{2} \left(1.0 - \frac{\mathbf{w}_i^T \cdot \mathbf{w}_j}{\|\mathbf{w}_i\| \|\mathbf{w}_j\|} \right) \right]^2$$

where k is the mini batch size and the two summations signify computing pairwise losses across all possible pairs. The vectors \mathbf{h}_i^1 and \mathbf{h}_j^1 represent the output vectors of H1 for sample \mathbf{x}_i and \mathbf{x}_j respectively. A lower value of L_1 is obtained when a high value of $1.0 - \frac{\mathbf{w}_i^T \cdot \mathbf{w}_j}{\|\mathbf{w}_i\| \|\mathbf{w}_j\|}$ results in a high value of $(\mathbf{h}_i^1 - \mathbf{h}_j^1)^T \cdot (\mathbf{h}_i^1 - \mathbf{h}_j^1)$ and vice-versa. Higher value of $1.0 - \frac{\mathbf{w}_i^T \cdot \mathbf{w}_j}{\|\mathbf{w}_i\| \|\mathbf{w}_j\|}$ is obtained when the samples are dissimilar, thus the hash codes should be pushed apart. Similarly, lower value of this term is obtained when the samples are similar and therefore the hash codes should be pushed closer.

Table 2. Mean Average Precision values of NUS-WIDE and MIR-FLICKR25k data-sets computed by considering the top 50,000 retrieved images.

Algorithm		NUS-WIDE				MIRFLICKR-25K			
		12bits	24bits	32bits	48bits	12bits	24bits	32bits	48bits
ITQ [13]	non-deep	0.5295	0.5227	0.4932	0.5275	0.6418	0.655	0.6253	0.6504
PCAH [30]	non-deep	0.4566	0.4209	0.4016	0.3971	0.6098	0.6033	0.6085	0.6169
LSH [4]	non-deep	0.3308	0.3682	0.3726	0.3918	0.5708	0.5885	0.5843	0.6015
DSH [19]	non-deep	0.5065	0.5118	0.4902	0.4807	0.6561	0.6593	0.644	0.6422
SpH [15]	non-deep	0.3829	0.3959	0.3907	0.3947	0.586	0.5785	0.5789	0.5789
SH [34]	non-deep	0.4503	0.4029	0.4006	0.3731	0.6251	0.6157	0.6044	0.596
AGH [26]	non-deep	0.535	0.5226	0.497	0.4791	0.6378	0.6484	0.6473	0.6346
DH [9]	deep	0.4036	0.3974	0.3932	0.4014	0.5833	0.5945	0.5932	0.5942
UH-BDNN [8]	deep	0.4982	0.4996	0.4823	0.4853	0.6324	0.6279	0.6274	0.6258
DeepBit [25]	deep	0.4225	0.4247	0.4359	0.431	0.5974	0.6032	0.6077	0.6115
Ours Baseline	deep	0.4809	0.475	0.4793	0.4702	0.6064	0.6087	0.6077	0.6098
Ours Proposed (UDHT)	deep	0.6258	0.6397	0.6606	0.647	0.687	0.695	0.6667	0.6621

Table 3. Mean Average Precision values of NUS-WIDE and MIR-FLICKR25k data-sets computed by considering the top 5,000 retrieved images

Algorithm		NUS-WIDE				MIRFLICKR-25K			
		12bits	24bits	32bits	48bits	12bits	24bits	32bits	48bits
ITQ [13]	non-deep	0.6329	0.6299	0.594	0.6478	0.6908	0.7064	0.6684	0.6996
PCAH [30]	non-deep	0.5766	0.5046	0.49	0.4904	0.643	0.6306	0.6372	0.6516
LSH [4]	non-deep	0.3501	0.4093	0.4169	0.4546	0.5736	0.6049	0.5954	0.6239
DSH [19]	non-deep	0.5919	0.5982	0.5713	0.5791	0.6955	0.7071	0.6834	0.6603
SpH [15]	non-deep	0.4645	0.4645	0.4465	0.4472	0.5966	0.5811	0.5828	0.579
SH [34]	non-deep	0.5623	0.5033	0.4896	0.4533	0.6605	0.6405	0.6291	0.6213
AGH [26]	non-deep	0.6551	0.6459	0.6274	0.6225	0.6862	0.7005	0.6998	0.6853
DH [9]	deep	0.4733	0.4601	0.462	0.4763	0.6033	0.6195	0.6135	0.618
UH-BDNN [8]	deep	0.5923	0.5915	0.5902	0.6097	0.6654	0.6684	0.6672	0.6699
DeepBit [25]	deep	0.5463	0.5548	0.5624	0.561	0.589	0.6027	0.609	0.6086
Ours Baseline	deep	0.6202	0.627	0.6247	0.6249	0.6365	0.6326	0.6373	0.6352
Ours Proposed (UDHT)	deep	0.6709	0.6805	0.6955	0.6763	0.7346	0.743	0.7034	0.7054

3.4.2 Mini-batch-wise Hinge Loss

In addition to the pairwise similarity loss, we also intend to back-propagate a loss that forms a semantic embedding space at the output of H2. Such a loss function adjusts the feature spaces of not only the H2 layer but also some of the previous layers (FC3, FC2), thus transmitting the semantic information from the tags back into the network. As H1 is connected to the output of FC3, the semantic information contained in FC3 will aid in learning the hashes at the output of H2, thus enhancing the model’s performance. To this end, we define the following loss,

$$L_2 = \sum_n \sum_{j \neq n} \max[0, \text{margin} + \mathbf{w}_j \cdot \mathbf{h}_n^2 - \mathbf{w}_n \cdot \mathbf{h}_n^2]$$

where \mathbf{h}_n^2 represents the output of the head H2 for the n^{th} sample in the mini-batch. The loss L_2 is 0 only when the quantity $\mathbf{w}_n \cdot \mathbf{h}_n^2$ is more than the quantity $\text{margin} + \mathbf{w}_j \cdot \mathbf{h}_n^2$. That is, the value of the loss is zero only when the prediction of head H2 for the n^{th} sample is closer to the ground truth aggregated tag vector \mathbf{w}_n than to any other ground truth tag vector \mathbf{w}_j by a margin margin . Note that, a similar idea was previously considered in [16], where the goal was to semantically embed videos onto a space using the *word2vec* representation of the video labels. As such, their approach is inherently supervised (i.e., assuming the label information).

3.4.3 Quantization Loss

Additionally, we impose the quantization loss on the H1 output in order to force the outputs to be close to 0 or 1.

It can be mathematically formulated as follows,

$$L_3 = - \sum_{i=1}^k \frac{1}{b} (\mathbf{h}_n^1 - 0.5\mathbf{I})^T \cdot (\mathbf{h}_n^1 - 0.5\mathbf{I})$$

This function penalizes the network if the output of a neuron is close to 0.5.

While training, we weigh the three loss components L_1 , L_2 and L_3 by factors λ_1 , λ_2 and λ_3 respectively. Therefore the resultant loss that will be back propagated is as follows,

$$L = \lambda_1 L_1 + \lambda_2 L_2 + \lambda_3 L_3$$

3.5. Building a Baseline

In addition to comparing our method with several unsupervised state-of-art models, considering that few models have explicitly used tags, we also built a baseline that employs the binary tag vectors. We, therefore, make slight modifications to our model to accommodate this scenario. Firstly, we suppose that two images are similar if both of them share at least one tag. Such kind of formulation has been used in various supervised learning methods where they consider two images to be similar if both of them share at least one label. Since our problem setting is unsupervised, we use tag vectors instead of label vectors. Tag vectors are binary vectors whose length is equal to the total number of tags in the data-set and will have a value of 1 if the tag is associated with the image and 0 otherwise.

Regarding the network architecture, only the head H1 is kept and H2 is completely removed. We do this owing to the fact that the real-valued vectors (like aggregated tag vectors in the above scenario) are not available in this case, to regress the outputs to. Additionally, in the previous case, the loss applied on H1, i.e., the L_1 component has a real-valued ground truth similarity, unlike the current scenario. Therefore, we use a different loss component (contrastive loss) to accommodate the binary valued ground truth similarity labels. The equation of the loss is as follows,

$$L_4 = \sum_{i=1}^k \sum_{j=1}^k S * (1 - \beta) * D + (1 - S) * \beta * (\max(0, \text{margin} - D))^2$$

$$\text{where } D = \frac{1}{b} (\mathbf{h}_i^1 - \mathbf{h}_j^1)^T \cdot (\mathbf{h}_i^1 - \mathbf{h}_j^1)$$

Here, *margin* represents the margin associated with the hinge loss component of the contrastive loss, S represents the ground truth similarity label, and β represents the fraction of similar sample pairs present in the mini batch. Weighing the loss sub-components by β and $1 - \beta$ respectively are important due to the fact that in any mini-batch only a small fraction of the image pairs will have at least

Table 4. Table representing the performance of the model by using the *mean* and *idf* aggregation functions; Mean Average Precision values for 12, 24, 32, 48 bit hash codes for the MIR-FLICKR25K dataset are reported

	12bits	24bits	32bits	48bits
<i>idf</i>	0.6602	0.6664	0.6687	0.6598
<i>mean</i>	0.687	0.695	0.6667	0.6621

one tag in common, thus making the dataset highly imbalanced. We therefore incorporate β weight factor in the loss. Thus the final loss for the baseline model becomes,

$$L = \lambda_3 L_3 + \lambda_4 L_4$$

4. Experiments and Results

4.1. Datasets

NUS-WIDE This is a Web image dataset with 269,648 images collected from Flickr. Each image is associated with a set of tags. [5] presents that there is a total of 425,059 tags associated with the 269k images. Further, the authors of [5] conducted manual annotation of these images to a predefined set of 81 labels. For our experiments, we used only the images that are associated with at least three of the 1000 most frequent tags and at least one of the 21 most frequent labels. Thus we formed a training set of 100,000 images and a testing set of 2,000 images. We used the whole training set as the database and the testing set as the query set during evaluation.

MIR-FLICKR25K This is a comparatively smaller dataset with 25,000 images collected from Flickr and contains 1386 tags associated with them. [17] manually associated the images with 38 semantic categories. For our experiments, we used the images which are associated with at least three tags and at least one of the 38 categories. Thus we used a total of 16,000 images for training and 2,000 for testing. For both the data-sets, we randomly picked the testing set without considering the labels of the images.

4.2. Training

We trained our model using mini-batch gradient descent with a learning rate of 0.001 for the last three layers (FC3, H1, and H2) and a learning rate of 0.0001 for the pre-trained layers (CONV1 - FC2). We also used the momentum term with the rate of momentum equal to 0.9. Additionally, the weighing factors for the loss, λ_1 , λ_2 , λ_3 and λ_4 , are set to 1.0, 10.0, 1.0 and 1.0 respectively for all the experiments. These values are determined by performing a grid search over the hyper-parameter space. Additionally, the *word2vec* model that we used was trained on 1 billion words from the Wikipedia documents and outputs a 300-dimensional vector

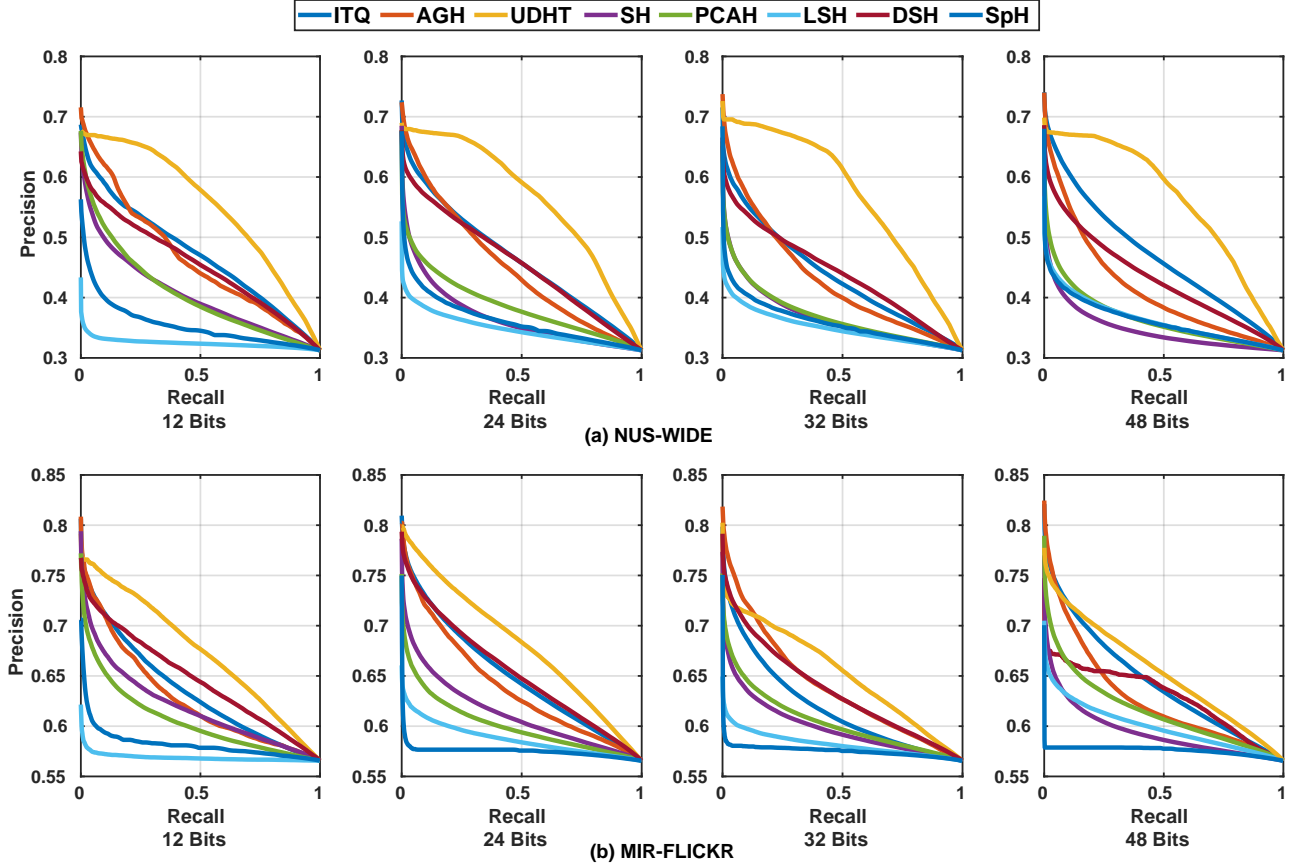


Figure 2. Precision Recall curves for NUS-WIDE and MIR-FLICKR datasets.

for a given word. Therefore the number of output neurons on H2 is set to 300.

4.3. Performance Evaluation

We evaluated the learned hash codes for the task of semantic image retrieval. We used the mean-Average-Precision (mAP) metric to compare our model’s performance to the existing methods. We used the same protocol used by [24], [33], [23] and several others to compute the mAP values. The results are compared against ten state-of-art approaches ITQ, PCAH, LSH, DSH, SpH, SH, AGH, DH, UH-BDNN and DeepBit hashing. All the methods are run using the code provided by the authors and for the suggested hyper-parameter settings. As most of the works presented here are based on the pre-determined feature vectors, we extracted the 4096-dimensional vectors from the AlexNet model (i.e the output of FC2) and used them as input to these methods.

We evaluated the performance of the model using the *mean* and the *idf* functions as the aggregation function on MIR-FLICKR data-set. We noticed that *mean* function seemed to work slightly better than the *idf* function in three of the four (12, 24, 32 and 48 bits) cases. Therefore, the

mean aggregation function was used for our proposed approach in all the experiments.

Further, we computed the mAP for two different settings, one using the top 50,000 retrieved images and another using the top 5,000 retrieved images in the training set and report the results in Table 1 and Table 2 respectively. The first seven methods presented here are non-deep-learning methods while the last three are deep-learning-based. Additionally, DH [9] and UH-BDNN [8], even though being deep-learning-based, depend on the hand-crafted features. DeepBit [25] is the only work that takes a raw image as input and produces a binary code, but its performance is inferior to most other methods. In contrast, our approach (UDHT) is an end-to-end framework and performed superior than all the state-of-art methods on both datasets.

The non-deep-learning based approaches ITQ [13] and AGH [26] seem to stand in the second and the third places in terms of the mAP values in the experiments. These methods are performing superior to the existing deep learning based methods ([9], [8], [25]) as well. Thus, the current state-of-art in unsupervised hashing is still non deep learning based. Through this paper, we set a new state-of-art in the area of unsupervised image hashing which is deep learning based.

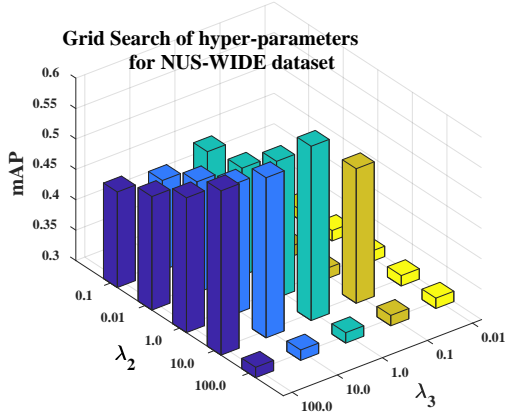


Figure 3. mAP values obtained for various settings of hyper-parameters for the NUS-WIDE dataset

Furthermore, our approach has the flexibility of choosing a different aggregation function that might best represent the tag-label relationship, thus leading to further higher mAP values.

We also noticed that the performance enhancement obtained for the NUS-WIDE data-set is higher as compared to the MIR-FLICKR25K data-set. This may be a consequence of the less amount of data available for training in the MIR-FLICKR data-set. Also, we observed that for any query image in the MIR-FLICKR data-set, 55% database images are “similar”, in the sense of sharing at least a common label. Since this sense of similarity was used to evaluate the algorithms, for any query image, even a random retrieval strategy would give a mAP value of 0.55. This number is around 0.35 for the NUS-WIDE data-set. This explains why mAP numbers in the mAP Tables are always above 0.35 and 0.55 on the two data-sets respectively. The number (0.55) seemed quite high for a retrieval evaluation data-set since in the real-world, given a random query image, the fraction of the images in the data-base that are semantically similar to the query image is quite low. We still use MIR-FLICKR data-set for our evaluation purposes due to the lack of better data-sets which have image-tag pairs.

For further analysis, we plotted the precision-recall curves for both the data-sets in figure 3. These curves are computed taking into consideration all the retrieved samples from the data-base for a given query image. More specifically, we computed the average precision for various values of recall (1000 discrete values of recall), for all query images and plotted them. The huge performance gain of our approach on the NUS-WIDE data-set can be noticed from these graphs as well.

4.4. Ablation Studies

The presence of three loss components in the objective functions triggers the obvious question of combining them

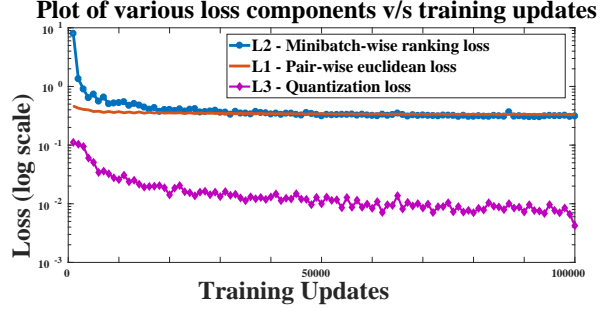


Figure 4. Evolution of the loss components v/s training updates

in the right proportions. To analyze this, we fix the value of λ_1 to 1.0 and change the values of λ_2 and λ_3 between 0.01 and 100.0. We performed a grid search over this range and chose the best hyper-parameters for our final model. Specifically, we set three values to the ones that gave maximum mAP value over a validation set during the grid search. For each setting of the hyper-parameter values, we only used 10,000 training sample due to the high training time of these experiments. A bar plot of the validation mAPs of NUS-WIDE dataset for various values of λ_2 and λ_3 is given in Figure 2. It can be noticed that higher values of λ_2 and lower values of λ_3 gave significantly better mAP as compared to other combinations. A similar behaviour was noticed on the MIR-FLICKR dataset as well. This is in accordance with the rationale presented in Section 3.3 (and as mentioned in [10]) that a ranking loss is better at forming semantically meaningful spaces as compared to Euclidean loss components. While this rationale is yet to be validated mathematically, our results suggest this seems to be the case from an empirical point of view.

Additionally, we plotted the training loss for each of the loss components for one of our experiments to give an understanding to the reader regarding how each of the loss components behaved as the training progressed. Figure 4 presents this plot. The losses are plotted after setting their corresponding weights ($\lambda_1, \lambda_2, \lambda_3$) to 1.0, 10.0, 1.0. We noticed that the network performed better when L_2 dominated during the initial training phase and becomes comparable to L_1 later during the training, than the case where both L_1 and L_2 are in the same order of magnitude since the beginning of training. It was also observed that a low value of L_3 leads to a better performance. We noticed that a previous work [36] also assigned small weight to the quantization term. This loose requirement on the weight of L_3 can be presumed due to the fact that, high L_3 values may lead to binary output values at H1 early in the training, leading to zero gradients, thus in turn leading to no weight updates.

5. Conclusion

We attempted the problem of unsupervised deep image hashing using the tag embedding. To our best knowledge, our method is the first end-to-end unsupervised hash learning algorithm that takes raw images as inputs and produces hash codes and performs on par with the state-of-art models for semantic image retrieval. In training, our model takes image-tag pairs as input. Therefore, our model is applicable to Web images where such information is abundant. Our results show significant performance boost when evaluated on two well-known datasets, as compared to the existing unsupervised methods. Our future work includes better aggregation schemes in the *word2vec* space that may lead to improved performance.

References

- [1] Y. Cao, M. Long, J. Wang, and S. Liu. Deep visual-semantic quantization for efficient image retrieval. In *CVPR*, volume 2, page 6, 2017.
- [2] Y. Cao, M. Long, J. Wang, Q. Yang, and P. S. Yu. Deep visual-semantic hashing for cross-modal retrieval. In *Proceedings of the 22nd ACM SIGKDD International Conference on Knowledge Discovery and Data Mining*, pages 1445–1454. ACM, 2016.
- [3] A. Chakrabarti, V. Satuluri, A. Srivathsan, and S. Parthasarathy. A bayesian perspective on locality sensitive hashing with extensions for kernel methods. *ACM Transactions on Knowledge Discovery from Data (TKDD)*, 10(2):19, 2015.
- [4] M. S. Charikar. Similarity estimation techniques from rounding algorithms. In *Proceedings of the thirty-fourth annual ACM symposium on Theory of computing*, pages 380–388. ACM, 2002.
- [5] T.-S. Chua, J. Tang, R. Hong, H. Li, Z. Luo, and Y. Zheng. Nus-wide: a real-world web image database from national university of singapore. In *Proceedings of the ACM international conference on image and video retrieval*, page 48. ACM, 2009.
- [6] A. Dasgupta, R. Kumar, and T. Sarlós. Fast locality-sensitive hashing. In *Proceedings of the 17th ACM SIGKDD international conference on Knowledge discovery and data mining*, pages 1073–1081. ACM, 2011.
- [7] J. Deng, W. Dong, R. Socher, L.-J. Li, K. Li, and L. Fei-Fei. Imagenet: A large-scale hierarchical image database. In *Computer Vision and Pattern Recognition, 2009. CVPR 2009. IEEE Conference on*, pages 248–255. IEEE, 2009.
- [8] T.-T. Do, A.-D. Doan, and N.-M. Cheung. Learning to hash with binary deep neural network. In *European Conference on Computer Vision*, pages 219–234. Springer, 2016.
- [9] V. Erin Liong, J. Lu, G. Wang, P. Moulin, and J. Zhou. Deep hashing for compact binary codes learning. In *Proceedings of the IEEE Conference on Computer Vision and Pattern Recognition*, pages 2475–2483, 2015.
- [10] A. Frome, G. S. Corrado, J. Shlens, S. Bengio, J. Dean, T. Mikolov, et al. Devise: A deep visual-semantic embedding model. In *Advances in neural information processing systems*, pages 2121–2129, 2013.
- [11] R. Girshick, J. Donahue, T. Darrell, and J. Malik. Rich feature hierarchies for accurate object detection and semantic segmentation. In *Proceedings of the IEEE conference on computer vision and pattern recognition*, pages 580–587, 2014.
- [12] X. Glorot and Y. Bengio. Understanding the difficulty of training deep feedforward neural networks. In *Proceedings of the Thirteenth International Conference on Artificial Intelligence and Statistics*, pages 249–256, 2010.
- [13] Y. Gong, S. Lazebnik, A. Gordo, and F. Perronnin. Iterative quantization: A procrustean approach to learning binary codes for large-scale image retrieval. *IEEE Transactions on Pattern Analysis and Machine Intelligence*, 35(12):2916–2929, 2013.
- [14] M. Gupta, R. Li, Z. Yin, and J. Han. Survey on social tagging techniques. *ACM Sigkdd Explorations Newsletter*, 12(1):58–72, 2010.
- [15] J.-P. Heo, Y. Lee, J. He, S.-F. Chang, and S.-E. Yoon. Spherical hashing. In *Computer Vision and Pattern Recognition (CVPR), 2012 IEEE Conference on*, pages 2957–2964. IEEE, 2012.
- [16] S.-H. Hu, Y. Li, and B. Li. Video2vec: Learning semantic spatio-temporal embeddings for video representation. In *Pattern Recognition (ICPR), 2016 23rd International Conference on*, pages 811–816. IEEE, 2016.
- [17] M. J. Huiskes and M. S. Lew. The mir flickr retrieval evaluation. In *Proceedings of the 1st ACM international conference on Multimedia information retrieval*, pages 39–43. ACM, 2008.
- [18] Q.-Y. Jiang and W.-J. Li. Deep cross-modal hashing. *CoRR*, 2016.
- [19] Z. Jin, C. Li, Y. Lin, and D. Cai. Density sensitive hashing. *IEEE transactions on cybernetics*, 44(8):1362–1371, 2014.
- [20] A. Krizhevsky, I. Sutskever, and G. E. Hinton. Imagenet classification with deep convolutional neural networks. In *Advances in neural information processing systems*, pages 1097–1105, 2012.
- [21] B. Kulis and T. Darrell. Learning to hash with binary reconstructive embeddings. In *Advances in neural information processing systems*, pages 1042–1050, 2009.
- [22] B. Kulis and K. Grauman. Kernelized locality-sensitive hashing. *IEEE Transactions on Pattern Analysis and Machine Intelligence*, 34(6):1092–1104, 2012.
- [23] H. Lai, Y. Pan, Y. Liu, and S. Yan. Simultaneous feature learning and hash coding with deep neural networks. In *Computer Vision and Pattern Recognition (CVPR), 2015 IEEE Conference on*, pages 3270–3278. IEEE, 2015.
- [24] W.-J. Li, S. Wang, and W.-C. Kang. Feature learning based deep supervised hashing with pairwise labels. *arXiv preprint arXiv:1511.03855*, 2015.
- [25] K. Lin, J. Lu, C.-S. Chen, and J. Zhou. Learning compact binary descriptors with unsupervised deep neural networks. In *Proceedings of the IEEE Conference on Computer Vision and Pattern Recognition*, pages 1183–1192, 2016.
- [26] W. Liu, C. Mu, S. Kumar, and S.-F. Chang. Discrete graph hashing. In *Advances in Neural Information Processing Systems*, pages 3419–3427, 2014.

- [27] J. Long, E. Shelhamer, and T. Darrell. Fully convolutional networks for semantic segmentation. In *Proceedings of the IEEE Conference on Computer Vision and Pattern Recognition*, pages 3431–3440, 2015.
- [28] T. Mikolov, K. Chen, G. Corrado, and J. Dean. Efficient estimation of word representations in vector space. *arXiv preprint arXiv:1301.3781*, 2013.
- [29] S. Sen, F. M. Harper, A. LaPitz, and J. Riedl. The quest for quality tags. In *Proceedings of the 2007 international ACM conference on Supporting group work*, pages 361–370. ACM, 2007.
- [30] J. Wang, S. Kumar, and S.-F. Chang. Semi-supervised hashing for large-scale search. *IEEE Transactions on Pattern Analysis and Machine Intelligence*, 34(12):2393–2406, 2012.
- [31] J. Wang, T. Zhang, N. Sebe, H. T. Shen, et al. A survey on learning to hash. *IEEE Transactions on Pattern Analysis and Machine Intelligence*, 2017.
- [32] K. Wang, Q. Yin, W. Wang, S. Wu, and L. Wang. A comprehensive survey on cross-modal retrieval. *arXiv preprint arXiv:1607.06215*, 2016.
- [33] X. Wang, Y. Shi, and K. M. Kitani. Deep supervised hashing with triplet labels. In *Asian Conference on Computer Vision*, pages 70–84. Springer, 2016.
- [34] Y. Weiss, A. Torralba, and R. Fergus. Spectral hashing. In *Advances in neural information processing systems*, pages 1753–1760, 2009.
- [35] X. Xu, F. Shen, Y. Yang, H. T. Shen, and X. Li. Learning discriminative binary codes for large-scale cross-modal retrieval. *IEEE Transactions on Image Processing*, 26(5):2494–2507, 2017.
- [36] H.-F. Yang, K. Lin, and C.-S. Chen. Supervised learning of semantics-preserving hash via deep convolutional neural networks. *IEEE transactions on pattern analysis and machine intelligence*, 40(2):437–451, 2018.
- [37] X. Zhu, L. Zhang, and Z. Huang. A sparse embedding and least variance encoding approach to hashing. *IEEE transactions on image processing*, 23(9):3737–3750, 2014.